Chemistry of Molybdenum. Part 7.[1] Reactivity of Terminal Oxo-ligands in *cis*-$[MoO_2(acda)_2]$ (Hacda = 2-aminocyclopent-1-ene-1-carbodithioic acid) Toward Proton- and Electron-donor Reagents. Synthesis, Redox Chemistry and Spectroscopic Characterisation of Neutral Seven-co-ordinate Catecholato and Aryldiazenido Compounds of Molybdenum†

Sujit Baran Kumar and Muktimoy Chaudhury*
Department of Inorganic Chemistry, Indian Association for the Cultivation of Science, Calcutta 700 032, India

The reactivity of co-ordinated oxo-ligands in *cis*-$[MoO_2(acda)_2]$ (Hacda = 2-aminocyclopent-1-ene-1-carbodithioic acid) toward proton- and electron-donor reagents has been investigated. Molybdenum(VI) compounds $[MoO(L)(acda)_2]$ (L = catecholate, **2a**; 4-*tert*-butylcatecholate, **2b**; 3,5-di-*tert*-butylcatecholate, **2c**; naphthalene-2,3-diolate, **2d**; or tetrachlorocatecholate, **2e** are obtained when catechols are used for oxo abstraction. Substituted phenylhydrazines on the other hand form non-oxodiazenido complexes $[Mo(N_2C_6H_4X\text{-}p)(acda)_3]$ (X = H, **3a**; Me, **3b**; or Cl, **3c**). The compounds have been characterised by electronic, IR and ESR spectroscopy and electrochemistry. In the visible region the electronic spectra are dominated by a strong ligand-to-metal charge-transfer (l.m.c.t.) band for both series of compounds. Their electrochemistry has been studied in dimethylformamide at a platinum electrode. For the catecholato compounds **2a–2e** a metal-based reduction (Mo^{VI}–Mo^{V}, E_{pc}) and a ligand-based oxidation (E_{pa}) each involving a single electron are observed. Substituents in the catecholato ring have a significant influence on the energy of the l.m.c.t. transitions (E_{op}) as well as on E_{pc} and E_{pa}. A linear relationship exists between E_{op} and ΔE(redox) where $\Delta E(\text{redox}) = E_{pc} - E_{pa}$. The oxidised species derived from the 0/1+ redox couple of the diazenido series **3a–3c** are ESR active with hyperfine spectra due to ^{95,97}Mo and ^{14}N couplings. The electron-transfer orbital in this case is believed to be metal based with sufficient mixing from the diazenido nitrogen orbital.

The ubiquitous molybdenum cofactor of oxotransferase molybdenum enzymes contains terminal oxo group(s).[2] Their presence is believed to be obligatory to enzyme activity.[3,4] Intensive efforts, many through model studies,[5–9] have since been made to understand the mechanism(s) of oxo-transfer reactions catalysed by these enzymes. In this laboratory, we have been engaged in the study of Mo–S chemistry.[1,10–14] Assorted molybdenum compounds in biologically relevant oxidation states have been synthesised using oxo-transfer reactions.

In this paper we report the reactivity pattern of the *cis*-dioxomolybdenum centre in $[MoO_2(acda)_2]$[13] (Hacda = 2-aminocyclopent-1-ene-1-carbodithoic acid, **1**) toward proton- and electron-donor agents. Various substituted catechols (H_2cat) have been used as proton-donor ligands. Compounds of the type $[MoO(cat)(acda)_2]$ **2a–2e** were obtained. Their spectroscopic and electrochemical properties are reported. Also presented is the reactivity of $[MoO_2(acda)_2]$ with *para*-substituted arylhydrazines which are known to function both as proton- and electron-donor reagents under suitable reaction conditions.[15–17] Aryldiazenido compounds of the type $[Mo(N_2C_6H_4X\text{-}p)(acda)_3]$ (X = H, **3a**; Me, **3b**; or Cl, **3c**) are obtained as main product. Their spectroscopic, ESR and electrochemical properties are also reported.

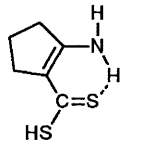

1

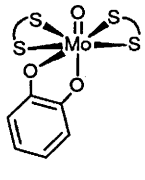

2

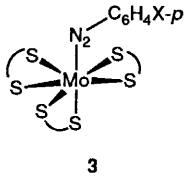

3

Experimental

Reagent-grade solvents, dried and distilled by standard methods,[18] were used in all cases. Reactions and manipulations of compounds were carried out under purified dinitrogen. Cyclopentanone (E. Merck), acetylacetone (BDH), phenylhydrazine (BDH) and triethylamine (E. Merck) were freshly distilled before use. Catechol (BDH) was recrystallised from benzene. Naphthalene-2,3-diol (Sigma), 4-*tert*-butylcatechol (Fluka), 3,5-di-*tert*-butylcatechol and tetrachlorocatechol (Aldrich), *p*-chlorophenylhydrazine hydrochloride and *p*-tolylhydrazine hydrochloride (Fluka) were used as received. All

† Abstracted in part from the Ph.D. Thesis of S. B. K., Jadavpur University, Calcutta, 1989.
Non-SI units employed: eV ≈ 1.60 × 10^{-19} J, G = 10^{-4} T.

other chemicals used for preparative work were of reagent grade and employed without further purification. The complex $[MoO_2(acda)_2]$ was prepared as described elsewhere.[13]

Physical Measurements.—Electrochemical techniques were carried out by using a Bioanalytical Systems CV-27 controller coupled with a Houston Instruments Omnigraphic 2000 X-Y recorder. For cyclic voltammetry, a platinum working electrode was employed with a saturated calomel electrode (SCE) as reference and a platinum counter electrode. Solutions were *ca.* 10^{-3} mol dm^{-3} in samples with 0.1 mol dm^{-3} tetra-*ethylammonium* perchlorate as supporting electrolyte in dimethylformamide (dmf, 10 cm^3). Electrochemically pure dmf was obtained from analytically pure solvent (Fluka, reagent grade) by using a procedure described in the literature.[19] For coulometry, a platinum-mesh 'flag' working electrode was used. All measurements were performed at ambient temperature (25 ± 2 °C) under an atmosphere of purified dinitrogen. Potentials are reported relative to the SCE and are uncorrected for liquid-junction potentials. Under the present experimental conditions the ferrocenium–ferrocene couple was located at +0.465 V.[20] X-Band ESR spectra in frozen solution (dmf–MeCN, 1:10 v/v) were recorded with an ER 200D-SRC Bruker spectrometer. The external magnetic field was controlled with an ER 042 MRH Bruker microwave bridge. The temperature was maintained with a Bruker ER 4111 VT device having an accuracy of ±1 K. Details of other physical measurements have been described elsewhere.[10–13] Elemental analyses (C, H and N) were made in this laboratory with a Perkin-Elmer 240C elemental analyser. Molybdenum contents were estimated gravimetrically as quinolin-8-olate.

Preparation of Compounds.—$[MoO(cat)(acda)_2]$ **2a** (cat = *catecholate*). In a three-necked flask equipped with a reflux condenser and a dropping funnel, $[MoO_2(acda)_2]$ (0.225 g, 0.5 mmol) was suspended in methylene chloride (20 cm^3). To this stirred suspension was added dropwise a filtered freshly prepared solution of catechol in methylene chloride (15 cm^3) over a period of 15 min. After ≈0.5 h the colour of the reaction mixture changed to dark green from its original maroon. The resulting mixture was warmed to 40 °C and stirred for 5 h. After cooling to room temperature, the dark green microcrystalline product was filtered off, washed with methanol and finally dried *in vacuo*. Yield: 0.22 g (81%).

The other catecholato compounds **2b–2e** were prepared similarly in 60–80% yields using essentially the same procedure, with the use of appropriate catechols. For the synthesis of **2c** and **2e**, methanol was used as solvent.

$[Mo(N_2C_6H_4Me\text{-}p)(acda)_3]$ **3b**. A solution of *p*-tolylhydrazine hydrochloride (95 mg, 0.6 mmol) in methanol (10 cm^3) was neutralised with the stoichiometric amount of triethylamine. This solution was then added dropwise over a period of 15 min to a stirred suspension of $[MoO_2(acda)_2]$ (0.225 g, 0.5 mmol) in methanol (30 cm^3). The reaction mixture was refluxed for 4 h and brown microcrystals separated. The product was isolated by filtration, washed with methanol (4 × 10 cm^3) and dried *in vacuo*. Yield: 0.13 g (37%).

The complexes $[Mo(N_2Ph)(acda)_3]$ **3a** and $[Mo(N_2C_6H_4Cl\text{-}p)(acda)_3]$ **3c** were obtained by following the same procedure, in yields of 40–45%.

Recrystallisations of the above compounds were not successful because of their poor solubility in common organic solvents, except dmf. Satisfactory analytical results were however obtained (Table 1).

Results and Discussion

Complexes **2a–2e**.—The complex *cis*-$[MoO_2(acda)_2]$ reacts with stoichiometric amounts of catechols, replacing one oxo group by a catecholato(2−) ligand, to form green compounds of composition $[MoO(cat)(acda)_2]$ **2** in high yields (60–80%)

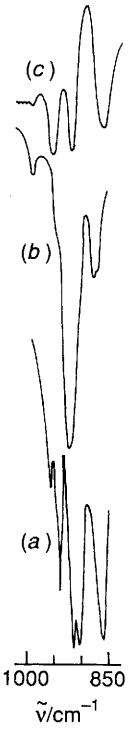

Fig. 1 Infrared spectra of (*a*) $[MoO_2(acda)_2]$, (*b*) $[MoO(O_2C_6H_4)(acda)_2]$ and (*c*) $[Mo(N_2C_6H_4Me\text{-}p)(acda)_3]$ showing stepwise elimination of oxygen atoms from the oxomolybdenum centre

according to equation (1). Compositionally similar seven-co-

$$[MoO_2(acda)_2] + H_2cat \longrightarrow [MoO(cat)(acda)_2] + H_2O \quad (1)$$

ordinated molybdenum compounds have been reported elsewhere.[21,22] Addition of excess of catechols is ineffective in replacing the second oxygen atom of the *cis*-dioxo starting compound. The catechols in this case are behaving as proton-donor reagents and the oxygen atom is removed from the metal co-ordination sphere by a simple acid–base type of reaction [equation (1)]. The molybdenum(VI) compounds **2a–2e** are all air stable in the solid state. They are diamagnetic and non-electrolytes with no detectable molar conductance in dmf.

A few characteristic infrared frequencies are listed in Table 1. The spectra of compounds **2a–2e** are dominated by a couple of strong absorption bands appearing at ≈1260 and 1470 cm^{-1}. These bands are also present in the spectra of the free catechol ligands. While the high-frequency band is assigned to a ring-breathing mode, the lower is due to the C–O stretching frequency, thus confirming the presence of a catecholate moiety in the molybdenum co-ordination sphere.[23] The remaining features are almost identical to those present in the spectrum of the precursor compound $[MoO_2(acda)_2]$[13] except in the 800–1000 cm^{-1} region where a strong sharp band (Fig. 1) is observed due to $\nu(Mo{=}O_t)$ vibrations. The compounds also contain a single sharp carbon–sulphur stretching mode at ≈815 cm^{-1} due to $\nu_{asym}(CSS)$, thus confirming the disulphur mode of chelation of acda.[10–13] The medium-intensity band at ≈340 cm^{-1} is due to $\nu(Mo{-}S)$ vibrations.[11,12]

The electronic absorption spectra of the catecholato complexes **2a–2e** are listed in Table 2. In the visible region, each compound exhibits (Fig. 2)* a single absorption band at *ca.* 550 nm. Since acda is not expected to be chromophoric in the visible region, these bands have been assigned as

* Spectra of complexes **2c–2e** are shown in Fig. 2. Those of the remaining catecholato compounds, **2a** and **2b**, have grossly identical features.

Table 1 Analytical and IR data for the complexes

	Analysis[a] (%)				IR[b]/cm^{-1}				
	Mo	C	H	N	ν(C–O)[c]	ν(ring breathing)[c]	ν_{asym}(CSS)[d]	ν(phenyl ring)[e]	ν(N=N)[e]
2a $[MoO(O_2C_6H_4)(acda)_2]$	17.8 (17.9)	39.7 (40.3)	3.7 (3.7)	5.2 (5.2)	1255	1470	815	—	—
2b $[MoO(O_2C_6H_3Bu^t\text{-}4)(acda)_2]$	16.3 (16.2)	44.6 (44.6)	4.8 (4.7)	4.7 (4.7)	1260	1470	818	—	—
2c $[MoO(O_2C_6H_2Bu^t_2\text{-}3,5)(acda)_2]$	14.8 (14.8)	48.0 (48.1)	5.6 (5.6)	4.3 (4.3)	1280	1470	818	—	—
2d $[MoO(O_2C_{10}H_6)(acda)_2]$	16.3 (16.4)	45.0 (45.0)	3.7 (3.7)	4.7 (4.8)	1260	1470	815	—	—
2e $[MoO(O_2C_6Cl_4)(acda)_2]$	14.2 (14.2)	32.1 (32.0)	2.4 (2.4)	4.2 (4.1)	1255	1475	818	—	—
3a $[Mo(N_2Ph)(acda)_3]$	14.3 (14.2)	42.7 (42.7)	4.2 (4.3)	10.3 (10.4)	—	—	820	760 700	1510
3b $[Mo(N_2C_6H_4Me\text{-}p)(acda)_3]$	14.0 (13.9)	43.3 (43.5)	4.5 (4.5)	10.1 (10.2)	—	—	815	750 700	1515
3c $[Mo(N_2C_6H_4Cl\text{-}p)(acda)_3]$	13.4 (13.5)	40.5 (40.6)	4.0 (3.9)	9.9 (9.9)	—	—	815	750 670	1500

[a] Calculated values are in parentheses. [b] As KBr disc. [c] From catecholato ligand. [d] From acda. [e] From aryldiazenido ligand.

Table 2 Electronic spectral data for $[MoO(cat)(acda)_2]$ complexes*

Complex	λ_{max}/nm (ε/dm^3 mol^{-1} cm^{-1})
2a	548 (5 400), 408 (46 900), 280 (28 200)
2b	564 (5 300), 406 (44 800), 280 (19 000)
2c	570 (4 300), 395 (43 000), 275 (20 600)
2d	538 (8 200), 390 (45 800), 327 (44 700), 260 (46 700)
2e	520 (7 500), 390 (34 300), 327 (55 300), 260 (32 000)

* Recorded in dmf.

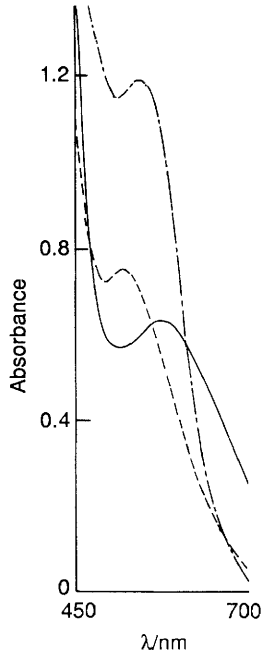

Fig. 2 Electronic absorption spectra of $[MoO(O_2C_6H_2Bu^t_2\text{-}3,5)(acda)_2]$ (——) (1.998 × 10^{-4} mol dm^{-3}), $[MoO(O_2C_6Cl_4)(acda)_2]$ (— — —) (2.003 × 10^{-4} mol dm^{-3}) and $[MoO(O_2C_{10}H_6)(acda)_2]$ (— - — - —) (2.045 × 10^{-4} mol dm^{-3}) in dmf solution

catechol(π) ⟶ Mo(d_π) ligand-to-metal charge-transfer (l.m.c.t.) transitions on the basis of their molar absorption coefficients (ε 4300–8200 dm^3 mol^{-1} cm^{-1}) and spectral shifts with various substituted catechols. The energy (E_{op}) of this charge-transfer band shows a gradual blue shift as the substituents in the catechol ring are varied from an electron-donating ($O_2C_6H_2Bu^t_2$-3,5) to an electron-withdrawing ($O_2C_6Cl_4$) type. Electron-donating substituents would be expected to raise the energy of the catecholate frontier orbitals and thus minimise the ligand-to-metal energy gap. Remaining bands in Table 2, appearing below or near 400 nm, are due to ligand-localised π–π* transitions.[11–13]

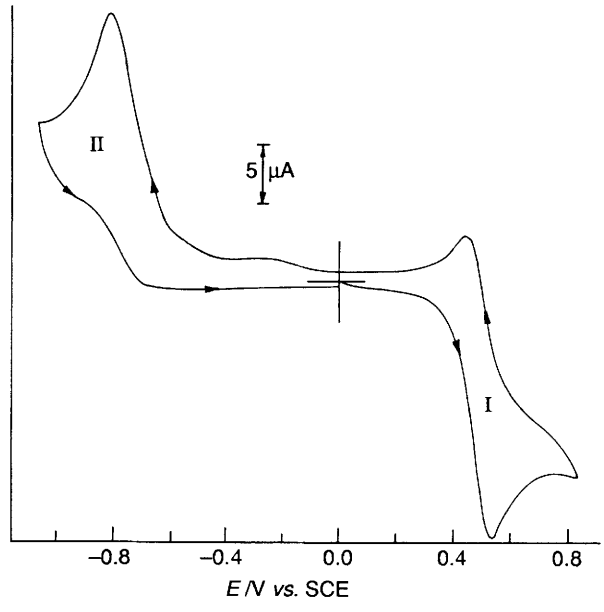

Fig. 3 Cyclic voltammogram (scan rate 50 mV s^{-1}) of $[MoO(O_2C_6H_2Bu^t_2\text{-}3,5)(acda)_2]$ (1.2 × 10^{-3} mol dm^{-3}) in dmf (0.1 mol dm^{-3} NEt_4ClO_4) at a platinum electrode

The electron-transfer behaviour of the catecholato compounds **2a**–**2e** according to cyclic voltammetry is summarised in Table 3. Each complex exhibits two redox processes within the potential range +1.0 to −1.0 V *vs.* SCE. The ligand Hacda is electrode inactive throughout the range of this investigation. In the anodic scan each of the compounds undergoes an oxidation (Process I) with varying degree of reversibility depending upon the type of substituents present in the co-ordinated catecholate ring. While for compounds containing electron-donating catechols (**2b** and **2c**) the oxidation process is perfectly reversible (Fig. 3),† an irreversible pattern is observed with **2a**, **2d**

† The electrochemical behaviours of **2a**, **2b**, **2d** and **2e** are not shown.

Table 3 Voltammetric[a] and spectral/electrochemical correlation data for $[MoO(cat)(acda)_2]$ complexes

	Ligand-centred oxidation (cat/sq)				Metal-centred reduction (Mo^{VI} to Mo^{V})		
Complex	E_{p_a}[b]	E_{p_c}[b]	$E_{\frac{1}{2}}$[b]	ΔE_p[c]	E_{p_c}[b]	E_{op}(l.m.c.t.)[d]/eV	ΔE(redox)[e]
2a	0.63	—	—	—	−0.83	2.262	−1.46
2b	0.58	0.50	0.54	80	−0.78	2.198	−1.36
2c	0.54	0.46	0.50	80	−0.84	2.175	−1.38
2d	0.82	—	—	—	−0.70	2.304	−1.52
2e	1.08	—	—	—	−0.56	2.384	−1.64

[a] Solvent dmf; supporting electrolyte NEt_4ClO_4 (0.1 mol dm^{-3}); sample concentration $\approx 10^{-3}$ mol dm^{-3}. [b] From CV using a scan rate of 50 mV s^{-1}; potentials are in volts *vs.* SCE. [c] $\Delta E_p = (E_{p_a} - E_{p_c})$ in mV. [d] From electronic spectra. [e] ΔE(redox) = $[E_{p_c}(Mo^{VI}\text{–}Mo^{V}) - E_{p_a}$(cat–sq)] in volts.

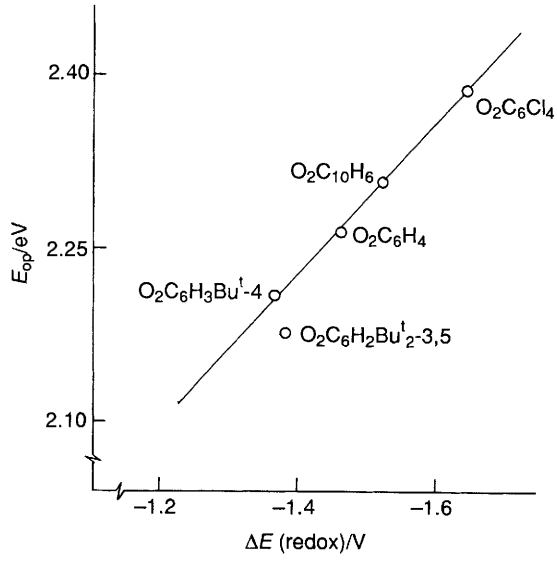

Fig. 4 Plot of ligand-to-metal charge-transfer energies (E_{op}) *vs.* ΔE(redox), the difference between the ligand (cat–sq) and metal (Mo^{VI}–Mo^{V}) centred redox potentials for the $[MoO(cat)(acda)_2]$ compounds

and **2e** where electron-withdrawing catechols are present. For molybdenum(VI) compounds, we believe this anodic process to be a ligand-based phenomenon resulting in oxidation of the co-ordinated catechol to the semiquinone (sq) stage [equation (2)]. It is the stability of the semiquinone radical cation that

$$[MoO(cat)(acda)_2] \rightleftharpoons [MoO(sq)(acda)_2]^+ + e^- \quad (2)$$

determines the reversibility of process I. Thus in compounds **2b** and **2c** the presence of Bu^t group(s) in the catechol ring efficiently stabilise(s) the cation radical possibly through a hyperconjugative effect. On the other hand the unsubsituted or tetrachloro catecholate complexes (**2a**, **2d** and **2e**) are oxidised irreversibly even at a high scan rate (500 mV s^{-1}) because of the lack of sufficient electron influx into the semiquinone ring which is probably needed for cation radical stabilisation.[22] The electron stoichiometry for process I has been established by constant-potential coulometric experiments. Exhaustive electrolysis past the oxidation process (at +0.75 V *vs.* SCE for **2c**) resulted in a charge transfer of 1.05 ± 0.07 F mol^{-1} of compound. Satisfactory coulometric results are also obtained with **2b**. Of note in Table 3 is an interesting trend in the catechol-centred oxidation of **2a**–**2e**. The potential (E_{p_a}) for this process is shifted to more positive values as the substituent(s) in the bound catechol ring becomes more electron withdrawing. This is as expected because oxidation in this case will be thermodynamically more facile when electron density flows into the catechol ring leading to stabilisation of the positive charge of the cation radical.

In the cathodic scan an irreversible reduction labelled as process II (Fig. 3) is obtained. The reduction potential (E_{p_c}) for this process shows a systematic shift to more negative values as the electron-donor capacity of the co-ordinated catechol increases (Table 3). We believe this cathodic process is due to a metal-centred electron transfer comprising molybdenum(VI) and -(V) states [equation (3)]. The lack of anodic response (Fig.

$$[Mo^{VI}O(cat)(acda)_2] + e^- \longrightarrow [Mo^{V}O(cat)(acda)_2]^- \quad (3)$$

3) even at a high scan rate (500 mV s^{-1}) is evidently due to rapid decomposition of the reduced molybdenum(V) species. Determinations of the electron stoichiometry for the redox couple (3) by constant-potential bulk electrolysis were not satisfactory because of continuous coulomb counts. Involvement of a single electron in process II is however established by comparing the observed current heights at E_{p_c} with the corresponding one-electron current parameters (E_{p_a}) of process I using the appropriate equation as reported elsewhere.[10]

Spectral and Electrochemical Correlations.—Electronic absorption spectroscopy and cyclic voltammetry in many cases are two complementary probes of charge-transfer processes within metal complexes. The l.m.c.t. band in the visible spectrum of $[MoO(cat)(acda)_2]$ arises from a cat(π) ⟶ Mo(d_π) transition, which is equivalent to oxidation of co-ordinated catechol (cat ⟶ sq) and reduction of the metal centre (Mo^{VI} ⟶ Mo^{V}) as shown in equation (4). The energy of this

$$[Mo^{VI}O(cat)(acda)_2] \xrightarrow[\text{l.m.c.t.}]{E_{op}} [Mo^{V}O(sq)(acda)_2]^* \quad (4)$$

l.m.c.t. transition (E_{op}) should in principle be related to the difference of two electrochemical potentials[24] [equation (5)]

$$E_{op}(\text{l.m.c.t.}) = E[Mo^{VI}(cat)\text{–}Mo^{V}(cat)] - E[Mo^{VI}(cat)\text{–}Mo^{VI}(sq)] + \kappa_i + \kappa_o$$
$$= \Delta E(\text{redox}) + \kappa_i + \kappa_o \quad (5)$$

where $E[Mo^{VI}(cat)\text{–}Mo^{V}(cat)]$ is the reduction potential of the molybdenum(VI) centre bound to catechol in $[MoO(cat)(acda)_2]$, $E[Mo^{VI}(cat)\text{–}Mo^{VI}(sq)]$ is the oxidation potential of the catechol ligand (cat/sq) bound to Mo^{VI} in the same series of compounds **2a**–**2e**, and ΔE(redox) is the difference between these two potentials; κ_i and κ_o are the inner (vibrational) and outer (solvation) reorganisation energies of the c.t. excited state.[24] Equation (5) has been applied to our system for which the reduction potentials (E_{p_c}) of the metal centre, oxidation potentials (E_{p_a}) of the ligand (catechol) centre and charge-transfer data (E_{op}) are all known (Table 3). The computer-

Table 4 Electronic spectra[a] and electrochemical[b] data for $[Mo(N_2C_6H_4X\text{-}p)(acda)_3]$ complexes

Complex	λ_{max}/nm (ε/dm^3 mol^{-1} cm^{-1})	$E_{\frac{1}{2}}$[c]/V	ΔE_p[d]/mV	i_{p_a}/i_{p_c}
3a	538 (5 150), 392 (33 000), 296 (21 000)	0.22	70	0.98
3b	540 (5 000), 390 (39 500), 295 (22 150)	0.18	80	1.02
3c	540 (5 200), 390 (27 000), 295 (20 700)	0.28	90	1.01

[a] In dmf. [b] Solvent dmf; supporting electrolyte NEt_4ClO_4 (0.1 mol dm^{-3}); complex concentration $\approx 10^{-3}$ mol dm^{-3}; working electrode Pt. [c] From CV using a scan rate of 50 mV s^{-1}; $E_{\frac{1}{2}} = 0.5\ (E_{p_a} + E_{p_c})$. [d] $\Delta E_p = E_{p_a} - E_{p_c}$.

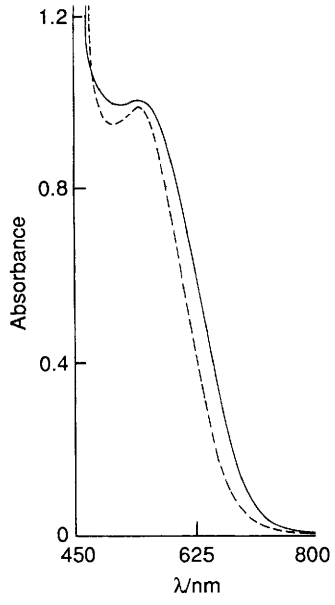

Fig. 5 Electronic absorption spectra of $[Mo(N_2C_6H_4Me\text{-}p)(acda)_3]$ (——) (2.189×10^{-4} mol dm^{-3}) and $[Mo(N_2C_6H_4Cl\text{-}p)(acda)_3]$ (— — —) (2.032×10^{-4} mol dm^{-3}) in dmf solution

drawn least-squares line (Fig. 4) is $E_{op} = 0.729\ \Delta E(\text{redox}) + 1.191$ eV with a correlation coefficient of 0.97. For compound **2c** with 3,5-di-*tert*-butylcatecholate as ligand a deviation from linearity has been observed. This is possibly due to a change in the reorganisation energies ($\kappa_i + \kappa_o$) for this catechol with two bulky substituents in the ring.

Complexes $[Mo(N_2C_6H_4X\text{-}p)(acda)_3]$ **3a–3c**.—The non-oxo diazenido molybdenum compounds **3** are obtained in moderate yields (35–45%) by treating a suspension of $[MoO_2(acda)_2]$ in methanol with monosubstituted arylhydrazines under reflux. In the solid state the diazenido compounds are all air stable and have poor solubility in common organic solvents, except dmf. They are all diamagnetic and behave as non-electrolytes in dmf.

Pertinent IR bands with probable assignments are listed in Table 1. The appearance of phenyl-ring vibrations in the region 670–760 cm^{-1} together with a strong band at *ca.* 1510 cm^{-1} due to $\nu(N{=}N)$[16,25] confirm the inclusion of the aryldiazenido group in the molybdenum co-ordination sphere. The absence of oxo group(s) is indicated by the lack of characteristic $\nu(Mo{=}O_t)$ vibrations in the 1000–850 cm^{-1} region (Fig. 1). Remaining important bands are characteristic of disulphur chelation from acda as discussed earlier. Their electronic spectra in dmf contain several absorption maxima (Table 4). The only lower-energy band with high molar absorption coefficient ($\varepsilon \approx 5000$ dm^3 mol^{-1} cm^{-1}) displayed by these compounds at ≈ 540 nm (Fig. 5) is assignable to a l.m.c.t. transition probably originating from the $Mo(N_2Ph)^{3+}$ functional unit.[16,25] Remaining bands appearing below 400 nm are due to internal-ligand transitions.

The electrochemical behaviour of diazenido compounds **3a–3c** in dmf solutions has been investigated. In the initial anodic scan each compound undergoes an oxidation step in the

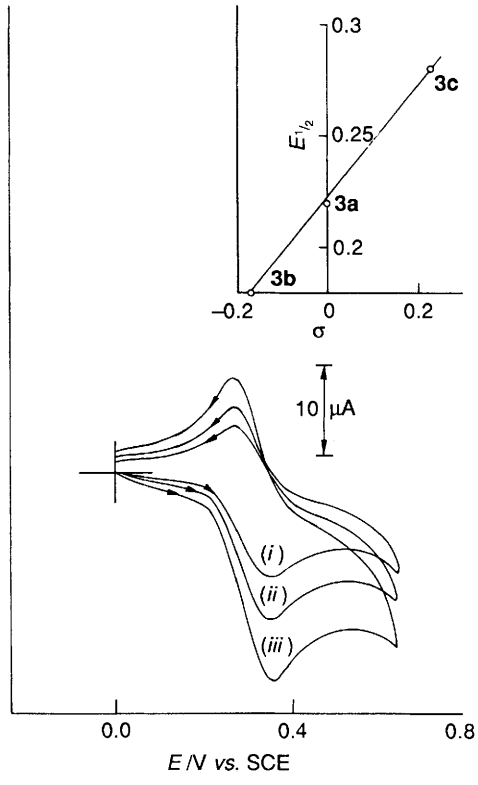

Fig. 6 Cyclic voltammograms of $[Mo(N_2C_6H_4Cl\text{-}p)(acda)_3]$ (0.83×10^{-3} mol dm^{-3}) in dmf (0.1 mol dm^{-3} NEt_4ClO_4) at a platinum electrode. Scan rates: 50 (*i*), 100 (*ii*) and 200 mV s^{-1} (*iii*). Inset: Hammett plot of $E_{\frac{1}{2}}$ against σ for complexes of the type $[Mo(N_2C_6H_4X\text{-}p)(acda)_3]$ [X = H, **3a**; Me, **3b**; or Cl, **3c**]

potential range 0 to +0.6 V (*vs.* SCE) which conforms to the criteria for Nernstian quasi-reversibility (ΔE_p increases slightly over the range of scan rates from 50 to 200 mV s^{-1}; the current function, $i_{p_a}/v^{\frac{1}{2}}$, is independent of scan rate and $i_{p_a}/i_{p_c} \approx 1$). A typical voltammogram exhibited by complex **3c** is shown in Fig. 6. Relevant electrochemical data are summarised in Table 4. The peak separations for this couple are reproducibly in the range 70–90 mV at a scan rate of 50 mV s^{-1} and are comparable to that of the ferrocenium–ferrocene couple (90 mV) under our experimental conditions, defining the observed voltammogram as a one-electron process [equation (6)]. The

$$[Mo(N_2C_6H_4X\text{-}p)(acda)_3] \overset{-e^-}{\rightleftharpoons} [Mo(N_2C_6H_4X\text{-}p)(acda)_3]^+ \quad (6)$$

electron stoichiometry for this process was further examined by constant-potential bulk electrolysis carried out at potentials 100 mV more positive than the respective E_{p_a} values. The anolyte changed in colour from brown to more darker shades. The results show that 1 mol of electrons is consumed per mol of compound.

The solution from the bulk electrolysis of complex **3b** was more fully characterised by ESR spectroscopy (Fig. 7). The one-electron oxidised species $[Mo(N_2C_6H_4Me\text{-}p)(acda)_3]^+$ in

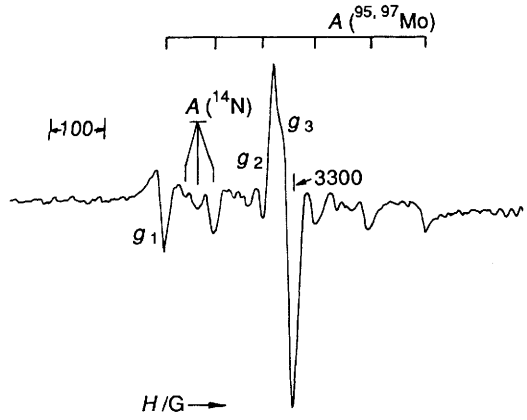

Fig. 7 X-Band frozen-solution ESR spectrum (80 K) of $[Mo(N_2C_6H_4\text{-}Me\text{-}p)(acda)_3]^+$ in dmf–MeCN (1:10 v/v) solution. Frequency, 9.1 GHz; gain, 8.0×10^3

frozen solution (80 K) shows a spectrum consistent with rhombic symmetry, with $g_1 = 2.126$, $g_2 = 1.999$ and $g_3 = 1.984$. The appearance of molybdenum hyperfine lines ($^{95,97}Mo$, $I = \frac{5}{2}$) in the spectrum confirms that the unpaired electron is located in a metal-based orbital. The high value of g_1 and the superhyperfine splitting due to ^{14}N ($I = 1$) coupling also confirm the mixing of the diazenido nitrogen orbital with the metal-centred redox orbital.

Correlation of Redox Potentials with Hammett Parameters.—Close inspection of Table 4 reveals an interesting trend in the redox potentials of the oxidation process. For compounds **3a**–**3c** the ease of oxidation of the metal centre increases (*i.e.* the energy of the highest occupied molecular orbital increases) as the substituent X in the diazenido aromatic ring becomes more electron donating. A more comprehensive pattern of $E_{\frac{1}{2}}$ variation becomes apparent from a plot of the Hammett constants of substituents against the $E_{\frac{1}{2}}$ of these compounds. A good linear fit (Fig. 6, inset) is obtained. This serves as an interesting example of the effect of remote substitution in controlling the electronic environment of the co-ordinated metal ion and is explicable in terms of resonance stabilisation of the oxidised cationic species by extended delocalisation of charge from the aromatic ring into the metal ion *via* the diazenido nitrogen atoms. One of the latter has direct access to the electron-transfer orbital of the metal as established by the appearance of superhyperfine lines due to ^{14}N coupling in the ESR spectrum of the oxidised **3b**.

Conclusion

The results described in this paper indicate that the oxo groups in the *cis*-$Mo^{VI}O_2$ moiety of a six-co-ordinate structure are relatively labile. One of them could be replaced by proton-donor reagents, *e.g.* catechols. The product is a seven-co-ordinate molecule containing a $Mo^{VI}O$ core. The oxygen atom of the latter species is substitutionally inert and needs an electron-donor reagent for its replacement.[26]

The nature of the co-ordinated catechols in $[MoO(cat)(acda)_2]$ **2a**–**2e** has a remarkable influence in controlling the electronic environment of the metal centre as reflected in the systematic variation of (*a*) the l.m.c.t. $[cat(\pi) \longrightarrow Mo(d_\pi)]$ band energies and (*b*) the redox potentials (E_{p_c} and E_{p_a}) of both the metal- and ligand-based electrochemical processes.

In the diazenido compounds **3a**–**3c** the formal oxidation state of molybdenum is not well understood.[25,27] Assuming a hydrazido to diazenido conversion, a two-electron process [equation (7)], one can conjecture that Mo^{VI} is probably

$$PhNHNH_2 \longrightarrow PhN_2^- + 2e + 3H^+ \qquad (7)$$

reduced to Mo^{IV} during the formation of compounds **3a**–**3c**. In that case we can explain the oxidation process [equation (6)] as due to a loss of an electron from a molybdenum(IV) species. The oxidised product being a monomeric molybdenum(V) species is therefore expected to show characteristic ESR activity. The appearance of superhyperfine lines due to ^{14}N coupling in the ESR spectrum (Fig. 7) confirms the electron-transfer orbital in this case to be metal based with sufficient mixing from the diazenido nitrogen orbital.

Acknowledgements

Thanks are due to Dr. Sanat K. Mandal of the Memorial University of Newfoundland for his help in electrochemical experiments.

References

1 Part 6, S. B. Kumar and M. Chaudhury, *J. Chem. Soc., Dalton Trans.*, 1991, 1149.
2 S. P. Kramer, J. L. Johnson, A. A. Ribeiro, D. S. Millington and K. V. Rajagopalan, *J. Biol. Chem.*, 1987, **262**, 16357; J. L. Johnson, N. R. Bastian and K. V. Rajagopalan, *Proc. Natl. Acad. Sci. USA*, 1990, **87**, 3190; S. P. Cramer, R. Wahl and K. V. Rajagopalan, *J. Am. Chem. Soc.*, 1981, **103**, 7721; S. P. Cramer, L. S. Solomonson, M. W. W. Adams and L. E. Mortenson, *J. Am. Chem. Soc.*, 1984, **106**, 1467.
3 R. Hille and V. Massey, in *Molybdenum Enzymes*, ed. T. G. Spiro, Wiley, New York, 1985, p. 443.
4 R. Hille and H. Sprecher, *J. Biol. Chem.*, 1987, **262**, 10914.
5 R. H. Holm and J. M. Berg, *Pure Appl. Chem.*, 1984, **56**, 1645.
6 R. H. Holm and J. M. Berg, *Acc. Chem. Res.*, 1986, **19**, 363.
7 J. P. Caradonna, P. R. Reddy and R. H. Holm, *J. Am. Chem. Soc.*, 1988, **110**, 2139.
8 J. A. Craig and R. H. Holm, *J. Am. Chem. Soc.*, 1989, **111**, 2111.
9 K. Wieghardt, M. Woeste, P. S. Roy and P. Chaudhuri, *J. Am. Chem. Soc.*, 1985, **107**, 8276.
10 S. B. Kumar and M. Chaudhury, *J. Chem. Soc., Dalton Trans.*, 1987, 3043.
11 M. Chaudhury, *Inorg. Chem.*, 1985, **24**, 3011.
12 M. Chaudhury, *Inorg. Chem.*, 1984, **23**, 4434.
13 M. Chaudhury, *J. Chem. Soc., Dalton Trans.*, 1984, 115.
14 M. Chaudhury, *J. Chem. Soc., Dalton Trans.*, 1983, 857.
15 A. Nakamura, M. Nakayama, K. Sugihashi and S. Otsuka, *Inorg. Chem.*, 1979, **18**, 394.
16 M. W. Bishop, G. Butler, J. Chatt, J. R. Dilworth and G. J. Leigh, *J. Chem. Soc., Dalton Trans.*, 1979, 1843.
17 P. L. Dahlstrom, J. R. Dilworth, P. Shulman and J. Zubieta, *Inorg. Chem.*, 1982, **21**, 933.
18 A. I. Vogel, *A Text-Book of Practical Organic Chemistry*, 3rd edn., Longman, London, 1973.
19 J. R. Bradbury, A. F. Masters, A. C. McDonell, A. A. Brunette, A. M. Bond and A. G. Wedd, *J. Am. Chem. Soc.*, 1981, **103**, 1959.
20 R. R. Gagnè, C. A. Koval and G. C. Lisensky, *Inorg. Chem.*, 1980, **19**, 2854.
21 J. R. Bradbury and F. A. Schultz, *Inorg. Chem.*, 1986, **25**, 4416.
22 S. Bristow, J. H. Enemark, C. D. Garner, M. Minelli, G. A. Morris and R. B. Ortega, *Inorg. Chem.*, 1985, **24**, 4070.
23 A. B. P. Lever, P. R. Auburn, E. S. Dodsworth, M. Haga, W. Liu, M. Melnik and W. A. Nevin, *J. Am. Chem. Soc.*, 1988, **110**, 8076.
24 E. S. Dodsworth and A. B. P. Lever, *Chem. Phys. Lett.*, 1986, **124**, 152; M. Haga, E. S. Dodsworth and A. B. P. Lever, *Inorg. Chem.*, 1986, **25**, 447.
25 H. Kang, S. Liu, S. N. Shaikh, T. Nicholson and J. Zubieta, *Inorg. Chem.*, 1989, **28**, 920.
26 S. B. Kumar and M. Chaudhury, unpublished work.
27 G. Butler, J. Chatt, G. J. Leigh and C. J. Pickett, *J. Chem. Soc., Dalton Trans.*, 1979, 113.

Received 4th December 1990; *Paper* 0/05456I